AD_____

Technical Report
69-80-AD

TWO-BODY TRAJECTORY ANALYSIS OF A PARACHUTE-CARGO AIRDROP SYSTEM

by

Maurice P. Gionfriddo

Project Reference:
1F162203D195

April 1969

Airdrop Engineering Laboratory
US ARMY NATICK LABORATORIES
Natick, Massachusetts 01760

FOREWORD

The work reported was performed by the author while attending the Center for Advanced Engineering Study at the Massachusetts Institute of Technology, Cambridge, Massachusetts, during the period February 1968 to February 1969. Funds were provided by a long-term training grant from the Department of the Army and by US Army Project No. 1F162203D195.

The author wishes to express his appreciation to Professors Eugene E. Covert and Eugene E. Larrabee of the M.I.T. Department of Aeronautics and Astronautics for their encouragement and guidance during this study.

TABLE OF CONTENTS

LIST OF FIGURES

ABSTRACT

Equations of motion for a three-degree-of-freedom, two-body airdrop system were derived and numerical solutions obtained by use of a digital computer. It was assumed that, for given initial conditions, the parachute drag area was a function of time only.

The results indicated that:

1. The derived equations of motion result in calculated trajectories which are good representations of actual airdrop trajectories.

2. The parameters which most affect altitude loss to equilibrium are parachute-cargo line length and parachute opening time.

3. There is an optimum parachute opening time which results in minimum altitude loss to equilibrium. Longer or shorter opening times will result in greater altitude losses to equilibrium.

4. Moderate variations of aircraft flight path inclination, initial cargo acceleration, and initial cargo velocity have only a small effect on altitude loss to equilibrium.

5. For a given equilibrium velocity, a cluster of small parachutes appears to be a better choice than a single large parachute for obtaining minimum altitude loss to equilibrium.

Introduction

The operational ability to successfully airdrop large cargoes from rear-loading aircraft flying at altitudes below 800 feet has been a Department of Defense goal for some years. This ability would greatly reduce the chance of aircraft detection by enemy surveillance devices and also increase airdrop accuracy by reducing the amount of time during which the parachute and cargo are subjected to the effects of the unpredictable winds. Efforts to achieve a low-altitude capability have been underway for some time but have not yet been completely fruitful.

Presently, the minimum airdrop altitude is determined almost entirely by the amount of altitude required for the airdrop system to reach equilibrium conditions: that is, when the cargo reaches terminal velocity and the parachute and cargo are in a vertical orientation. Thus, decrease in airdrop altitude can occur only by decreasing the vertical distance required to attain equilibrium conditions. Typical solutions to this problem have provided aerodynamic or mechanical means to decrease the opening times of the parachutes. This, of course, results in the full drag area of the parachute being applied earlier in the trajectory. This approach appears to be based on the rationale derived from consideration of the trajectory of a point-mass, i.e., the greater the decelerating force, the less altitude required to reach equilibrium. However, in an airdrop of a cargo from 800 feet altitude, a typical

distance between the parachute and cargo centers-of-gravity is on the order of 150 feet. As might then be expected, measured flight trajectories of parachute-cargo airdrop systems are quite different from point-mass trajectories. Thus, basing airdrop system designs on the characteristics of point-mass trajectories may not be a logical approach and may not result in the desired improvements in system performance.

Analyses to determine the trajectories of two-body parachute-cargo airdrop systems have been conducted [1,2,3]. The analyses of references 1 and 2 were used as bases for the development of a specific low-altitude cargo airdrop system which did not deviate too greatly from standard airdrop systems. As a result, the analyses were not of sufficient scope to determine basic differences in the response of point-mass and two-body systems to variations in system characteristics. The analysis of reference 3 was conducted primarily to determine the forces being exerted on the cargo and the motion of the cargo itself about its own center of gravity.

In a preliminary study by the author (results unpublished), equations of motion were solved with the assumptions that the parachute drag area and parachute mass were constant throughout the trajectory. These are not very realistic assumptions for the transient portion of the trajectory, but the calculated trajectories were similar enough to actual trajectories to provide a reasonable basis for determining trends. The conclusions derived from this preliminary study were encouraging

enough to spur on additional study. The results of this additional study are described in this report.

Theory

The airdrop system model used as a basis for the equations of motion is shown in Figure 1.

As usual in an analysis of this type, a number of assumptions were made to yield tractable solutions. The major assumptions are:

1. The airdrop method chosen is that of extraction by recovery parachute. In this method, the reefed recovery parachute is used to extract the cargo from the aircraft. After the cargo clears the aircraft, the reefing line is severed and the parachute is allowed to inflate. In this study, zero time coincides with the instant that the cargo leaves the aircraft and the parachute begins inflating from its reefed configuration.

2. The only aerodynamic forces acting on the parachute and cargo are drag forces.

3. The parachute and cargo drag coefficients are independent of their respective angles of attack.

4. The elastic line joining the parachute and cargo has a spring constant, k.

5. The parachute center of gravity is located at a fixed distance from its skirt regardless of the change in parachute shape as it opens.

6. The air density remains constant throughout the trajectory.

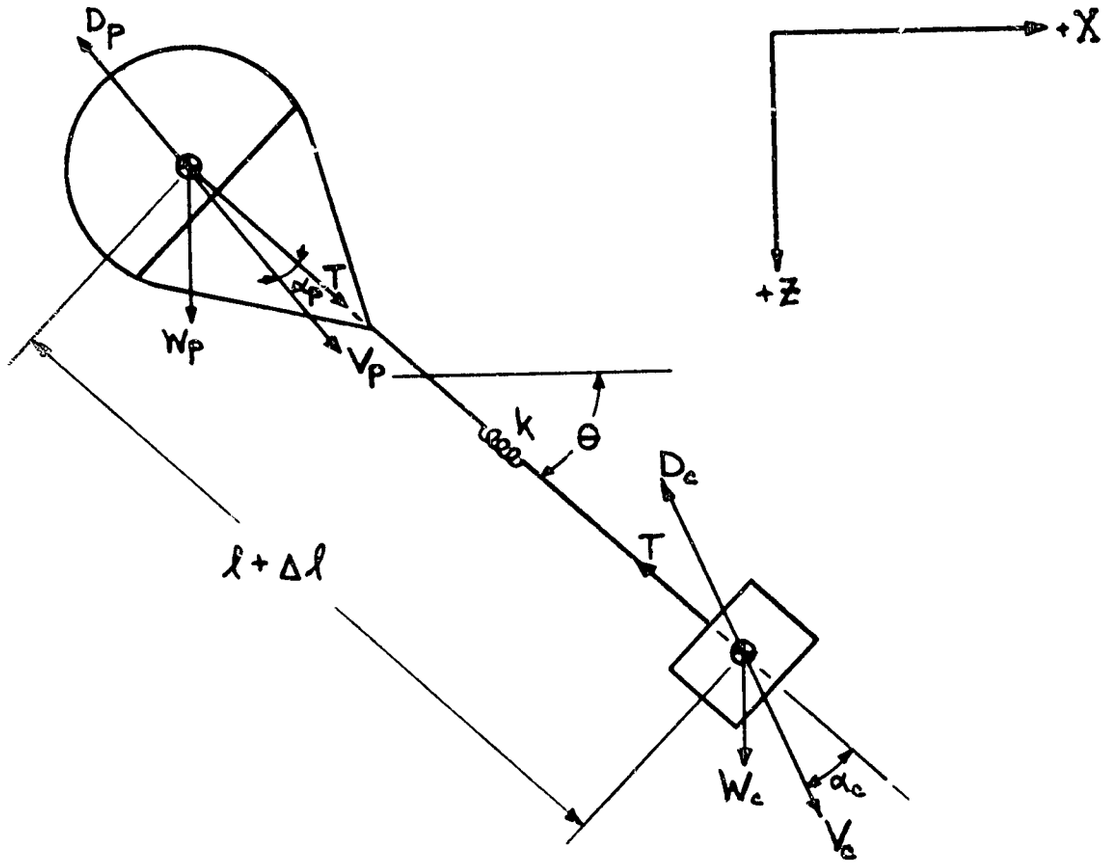

FIGURE 1 - PARACHUTE-CARGO GEOMETRY

These assumptions still permit rather general application of the equations of motion. The following additional assumptions, necessary to obtain numerical solutions, generate particular solutions to the equations which are then less general in application:

1. The variation in parachute area, S_p, for any given case, is a function of time only and is described by the following equation:

$$S_p = S_{p_o}\left[.0020 + .0034(118.4)^{\frac{t+t_r}{t_f}}\right] \qquad (1)$$

This equation is essentially that derived experimentally by Berndt and DeWeese[4] for a solid flat-circular canopy in its latter stages of opening, i.e., from $t/t_f = 0.3$ to $t/t_f = 1.0$. The constant, 0.0020, in the above equation differs from the constant, 0.0117, in Berndt and DeWeese's equation to take into account the fact that equation (1) was used, in this study, throughout the opening process, i.e., from $t/t_f = 0$ to $t/t_f = 1.0$. This was done to simplify the computer solution, but is not unreasonable since the reefed parachute shape is close to the shape assumed by Berndt and DeWeese for the beginning of the "terminal filling period".

2. From case to case, the variation in parachute opening time is inversely proportional to the initial cargo velocity.

3. Throughout the opening process, the shape of the parachute is represented by an inverted conical frustum topped by an oblate hemispheroid. (See Figure 2) The constants and equations used to relate these geometrical figures to the

parachute shapes were obtained from referenced data[5].

4. The parachute drag coefficient is constant throughout the opening process and for this study was chosen to be 0.7. This value is a compromise that attempts to take into account the variation in drag coefficient with velocity. This variation, calculated from referenced data [6] is shown in Figure 3.

Use of the theory by French [7] that the variation in parachute area during opening is not a function of time, but rather of distance along the trajectory was considered, but had to be discarded because of computer memory limitations.

Derivation of Equations

Summing forces along and perpendicular to the cargo and parachute velocity vectors, respectively, resulted in the following equations:

$$-\frac{m_c}{S_{D_c}} V_c^2 - T\cos\alpha_c + m_c g \sin(\theta+\alpha_c) = m_c \frac{dV_c}{dt} \qquad (2)$$

$$T\sin\alpha_c + m_c g\cos(\theta+\alpha_c) = m_c V_c \frac{d}{dt}(\theta+\alpha_c) \qquad (3)$$

$$-\frac{\rho}{2} C_{D_p} S_p V_p^2 + T\cos\alpha_p + m'_p g \sin(\theta+\alpha_p) = m_p \frac{dV_p}{dt} \qquad (4)$$

$$-T\sin\alpha_p + m'_p g\cos(\theta+\alpha_p) = m_p V_p \frac{d}{dt}(\theta+\alpha_p) \qquad (5)$$

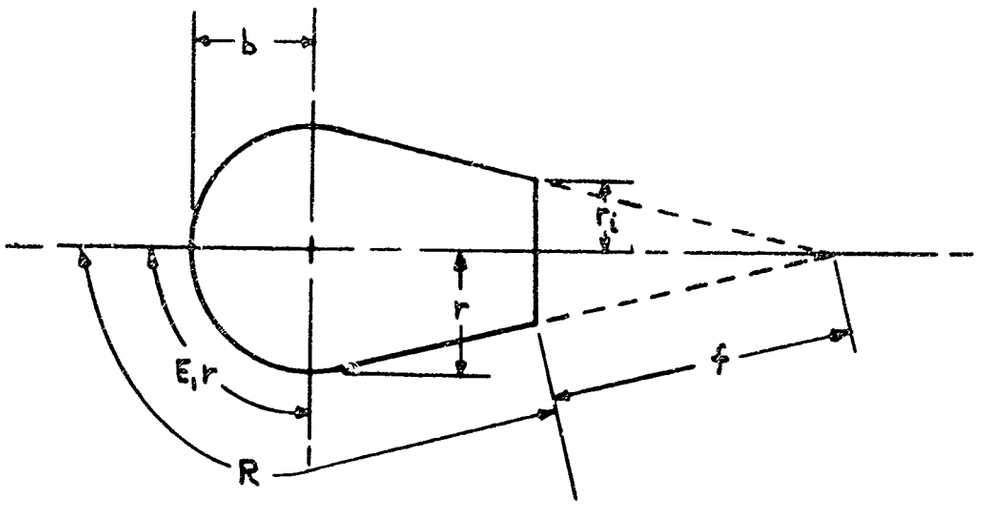

FIGURE 2 - SIMPLIFIED PARACHUTE SHAPE

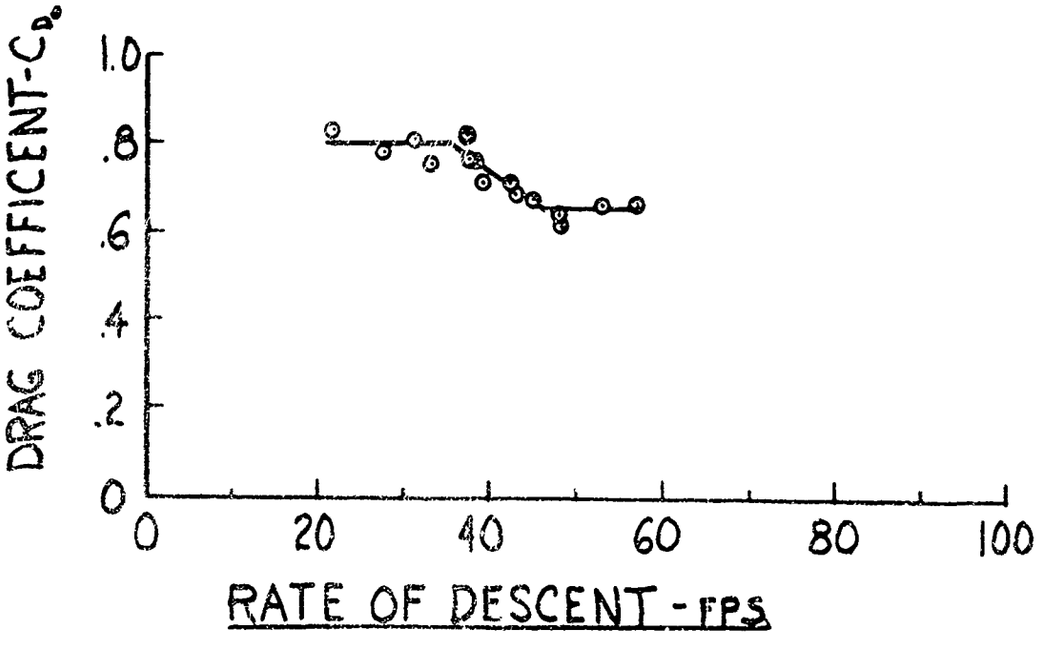

FIGURE 3 - PARACHUTE DRAG COEFFICIENT VERSUS RATE OF DESCENT

where

$$m_p = m'_p + (1+\kappa)\, m_{ia}$$

$$S_D = \frac{2m}{\rho S C_D}$$

The parameter, S_D, is known as the aerodynamic penetration [8] and is the distance an object of mass, m, travels in air of density, ρ, for aerodynamic drag proportional to the square of the speed to reduce its speed by a factor of e.

Another equation was determined by consideration of the effect of system geometry on the parachute and cargo velocities. The velocity components of the parachute and cargo in the direction of the line joining them are equal. Therefore, their relative velocity is the difference of their velocity components perpendicular to the line joining them [9]. It is this relative velocity which produces system rotation characterized by the following equation:

$$\frac{d\theta}{dt} = \frac{1}{l+\Delta l}\left(V_c \sin\alpha_c - V_p \sin\alpha_p\right) \qquad (6)$$

Equations ( ) through (5) are functions of the tension, T, in the line joining the parachute and cargo. The tension is a function of the distance between the parachute and cargo and is determined by the following equation:

$$T = k\left\{\left[(x_c - x_p)^2 + (z_c - z_p)^2\right]^{1/2} - l\right\} \qquad (7)$$

Additional equations are determined from consideration of the parachute and cargo velocity components in the x and z directions:

$$\frac{dx_c}{dt} = V_c \cos(\theta + \alpha_c) \tag{8}$$

$$\frac{dx_p}{dt} = V_p \cos(\theta + \alpha_p) \tag{9}$$

$$\frac{dz_c}{dt} = V_c \sin(\theta + \alpha_c) \tag{10}$$

$$\frac{dz_p}{dt} = V_p \sin(\theta + \alpha_p) \tag{11}$$

The equation for the time variation of the mass of included air in the parachute, m_{ia}, was derived using the method of reference 5 as follows (See Figure 2):

$$m_{ia} = \rho \, Vol._{canopy}$$

$$m_{ia} = \rho \left(Vol._{o.H.} + Vol._{c.F.} \right)$$

$$m_{ia} = \rho \frac{\pi}{3} \left[2r^3 \sqrt{1 - e_p^2} + \left(\frac{r^3 - r_i^3}{r_i} \right) \sqrt{r^2 - r_i^2} \right] \tag{12}$$

where:

$$r = \sqrt{S_p / \pi} \qquad r_i = \frac{f r}{R - 1.32 r + f} \qquad e_p = \frac{\sqrt{r^2 - b^2}}{r}$$

Equations (1) through (12) completely describe the problem and a solution can be determined using numerical techniques.

Non-dimensionalizing

Prior to solving the equations, the parameters were non-dimensionalized by the following method:

1. All lengths or distances were divided by S_{De}. Thus $X_c = x_c / S_{De}$.
2. All areas were divided by S_{De}^2.
3. Velocities were divided by V_e.
4. Non-dimensional time, τ, = $V_e t / S_{De}$.
5. Masses were divided by ρS_{De}^3.

Where S_{De} is the aerodynamic penetration of the parachute-cargo combination at equilibrium and V_e is the equilibrium velocity (terminal velocity) of the parachute-cargo combination. V_e and S_{De} are related by the following expression:

$$V_e = \sqrt{g \epsilon S_{De}}$$

The final non-dimensional equations of motion are as follows:

$$\frac{dV_c}{d\tau} = \frac{1}{\epsilon} \sin\phi_c - \frac{S_{De}}{S_{Dc}} V_c^2 - \left(\frac{k S_{De}}{m_c g \epsilon}\right) \sqrt{\cos\alpha_c} \qquad (13)$$

$$\frac{d\phi_c}{d\tau} = \frac{1}{V_c}\left[\frac{1}{\epsilon}\cos\phi_c + \left(\frac{k S_{De}}{m_c g \epsilon}\right) \sqrt{\sin\alpha_c}\right] \qquad (14)$$

$$\frac{d\alpha_c}{d\tau} = \frac{d\phi_c}{d\tau} - \frac{d\theta}{d\tau} \qquad (15)$$

$$\frac{dV_p}{d\tau} = \frac{1}{M_p}\left[-\frac{C_{D_p} S_p}{2} V_p^2 + \frac{M_p}{\epsilon}\sin\phi_p + \left(\frac{k}{\rho g \epsilon S_{D_e}^2}\right)\Gamma\cos\alpha_p\right] \quad (16)$$

$$\frac{d\phi_p}{d\tau} = \frac{1}{M_p V_p}\left[\frac{M'_p}{\epsilon}\cos\phi_p - \left(\frac{k}{\rho g \epsilon S_{D_e}^2}\right)\Gamma\sin\alpha_p\right] \quad (17)$$

$$\frac{d\alpha_p}{d\tau} = \frac{d\phi_p}{d\tau} - \frac{d\theta}{d\tau} \quad (18)$$

$$\frac{dX_c}{d\tau} = V_c\cos\phi_c \quad (19)$$

$$\frac{dX_p}{d\tau} = V_p\cos\phi_p \quad (20)$$

$$\frac{dZ_c}{d\tau} = V_c\sin\phi_c \quad (21)$$

$$\frac{dZ_p}{d\tau} = V_p\sin\phi_p \quad (22)$$

$$\frac{d\theta}{d\tau} = \frac{1}{(L+\Gamma)}\left[V_c\sin\alpha_c - V_p\sin\alpha_p\right] \quad (23)$$

$$\Gamma = \left\{\left[(X_c - X_p)^2 - (Z_c - Z_p)^2\right]^{1/2} - L\right\} \quad (24)$$

where:

$$\epsilon = \frac{m_c}{m_c + m_{la_e}} \qquad \phi = \theta + \alpha$$

Computation

The non-dimensional equations of motion were solved numerically using the Runge-Kutta-Gill [10] method on an IBM 1130 Digital Computer with both graphical and digital output. The equations were solved for 58 different sets of input values which are tabulated in Table 1.

Case 1 is a reasonable approximation of a typical airdrop where a 3250-lb. cargo is airdropped from an aircraft flying at an airspeed of approximately 130 knots and using a 100-ft. diameter parachute for extraction and recovery. The remaining cases constitute a systematic variation in the airdrop parameters considered most significant.

In each case, the trajectory solution was carried out to an arbitrary equilibrium condition which was defined as the time when the parachute-cargo orientation is within 5 degrees of vertical and, simultaneously, the cargo velocity is less than 1.05 times the equilibrium velocity.

The time increments used resulted in each trajectory being defined by at least 35 calculated points for the shorter trajectories and more than 250 calculated points for the longer trajectories.

Table I - Summary of Initial Conditions and Airdrop System Characteristics

Case No.	W_c lbs.	C_{D_c}	S_c ft.^{2}	W'_p lbs.	μ	$C_{D_{P_o}}$	D_{P_o} ft	V_a fps	V_r fps	ϕ_o deg.	ℓ_r ft.	k lbs./ft.	ℓ ft.	t_f sec.	f ft.	Δt sec.	Calculated Parameters S_{D_e} - ft.	Calculated Parameters V_e - fps
1	3250	1.0	72	250	0	0.7	100	220	40	0	19	1110	140	7.0	95	0.2	42.21	22.8
2													70					
3													55					
4													40					
5													35					
6													20					
7													1					
8													50					
9													65					
10													100					
11													80					
12													80	3.0				
13													80	5.0				
14													80	9.0				
15													80	11.0				

Table I - Continued

Case No.	W_c lbs.	C_{D_c}	S_c ft.^{2}	W'_p lbs.	μ	$C_{D_{P_o}}$	D_{P_o} ft	V_a fps	V_r fps	ϕ_o deg.	l_r ft.	k lbs./ft.	l ft.	t_f sec.	f ft.	Δt sec	Calculated Parameters S_{D_e} - ft.	Calculated Parameters V_e - fps
16													80	13.0				
17														11.0				
18														16.0				
19														9.0				
20														13.0				
21													90					
22													120					
23													220					
24										30								
25										-30								
26	32,500			2000			283				54		220				81.77	25.2
27	32,500			2000			283				54		220	10.0			81.77	25.2
28	32,500			2000			283				54		220	13.0			81.77	25.2
29	32,500			2000			283				54		220	16.0			81.77	25.2
30								110						18.0				

Table I - Continued

Case No.	W_c lbs.	C_{D_c}	S_c ft^2.	W'_p lbs.	μ	$C_{D_{P_o}}$	D_{P_o} ft.	V_a fps	V_r fps	ϕ_o deg.	l_r ft.	k lbs./ft	l ft.	t_f sec.	f ft.	Δt sec	Calculated Parameters S_{D_e} - ft.	Calculated Parameters V_e - fps
31								330						4.3				
32									20					6.3				
33									80					9.0				
34										15								
35										-15								
36									30					6.6				
37									60					7.9				
38								440						3.2				
39									50					7.4				
40	32,500			2000			283				54		220	20.0			81.77	25.2
41											13							
42											27							
43											35							
44					.25													
45											5							

Table I - Concluded

Case No.	W_c lbs.	C_{D_c}	S_c ft²	W'_p lbs.	μ	$C_{D_{po}}$	D_{po} ft.	V_a fps	V_r fps	ϕ_o deg	ℓ_r ft.	k lbs./ft.	ℓ ft.	t_f sec.	f ft.	Δt sec.	Calculated Parameters S_{D_e} - ft.	Calculated Parameters V_c fps
46													42.2	4.0				
47													42.2	6.0				
48													42.2	8.0				
49													220	16.0				
50													220	20.0				
51													220	24 0				
52													42.2	2.2				
53													42.2	3.0				
54													220	18.0				
55													42.2	3 6				
56													220	12.0				
57													220	14.0				
58	32,500			2000			283				54		220	22.0			81.77	25.2

Blanks indicate values are the same as Case 1

Results and Discussion

The trajectory obtained for Case 1, the nominal case, is shown in Figure 4. Included in the figure for comparison is a trajectory obtained from an actual flight test with initial conditions and system characteristics generally similar to those of Case 1. Unfortunately, the flight test data were not complete enough to insure that all conditions for the calculated and actual trajectories were identical. Also, actual trajectories are determined relative to the ground, while the calculated trajectories are determined relative to the air mass. Thus, the local winds will result in discrepancies between the two trajectories.

On this basis, the close similarity between the trajectories indicates that the equations do predict cargo trajectories reasonably well.

Figure 5 shows the variation in altitude loss to equilibrium with parachute-cargo line length, L . The trajectories for those cases with L less than 1.5 are characterized by asymptotic approaches to the vertical (θ = 90 deg.). For those cases with L greater than 1.5, the trajectories oscillate about the vertical and as L increases the oscillations become more pronounced. For those cases with L greater than 2, the scattering of points is caused by the fact that equilibrium is defined as a range of allowable values for θ and V_c . Because of the oscillations, the equilibrium conditions can be approached from either boundary of that range; that is, during that part of the oscillation where V_c is less than 1.05, θ can reach equilibrium by approaching the 85 degree boundary from

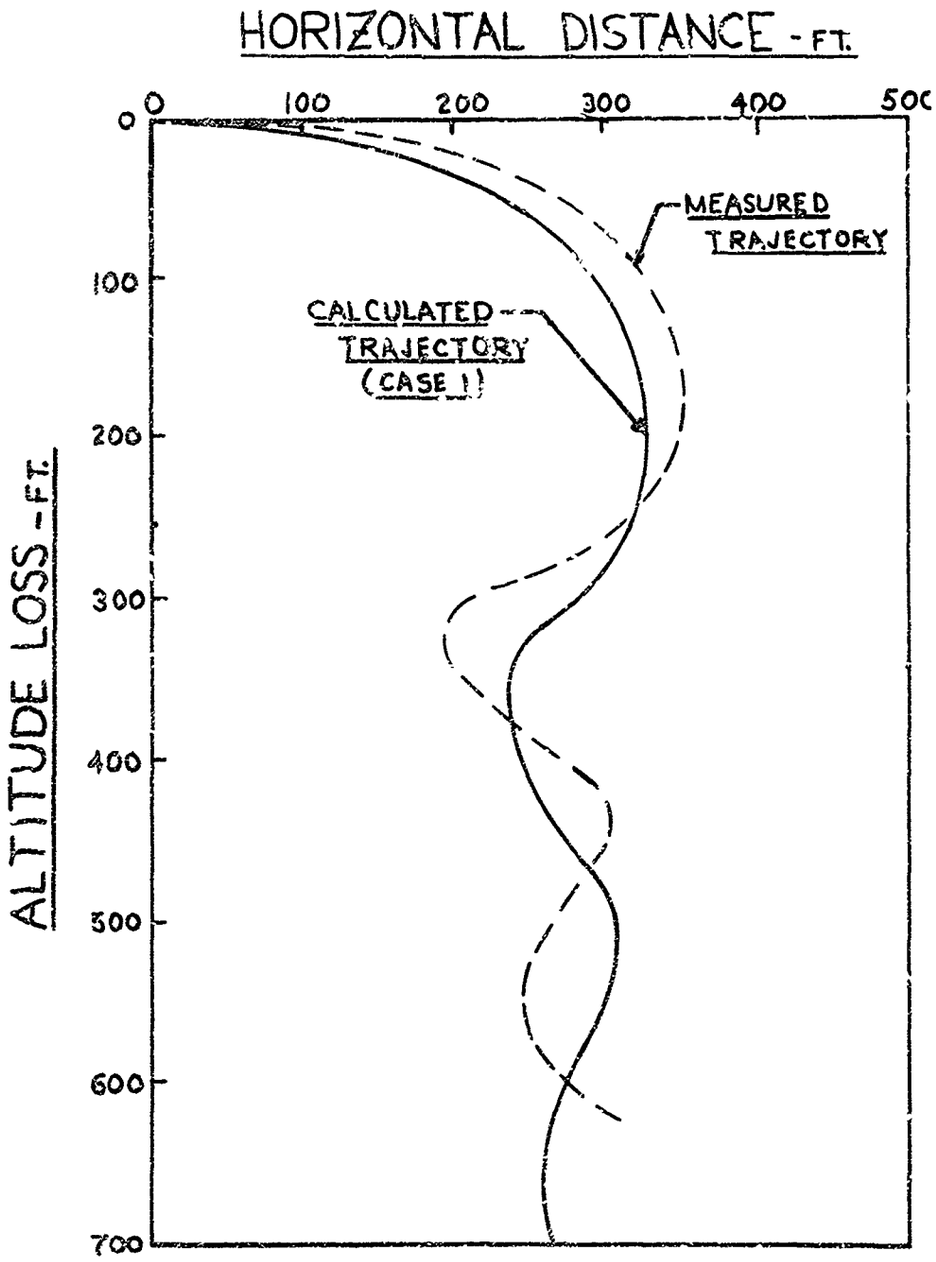

FIGURE 4 - COMPARISON OF CALCULATED AND MEASURED CARGO TRAJECTORIES

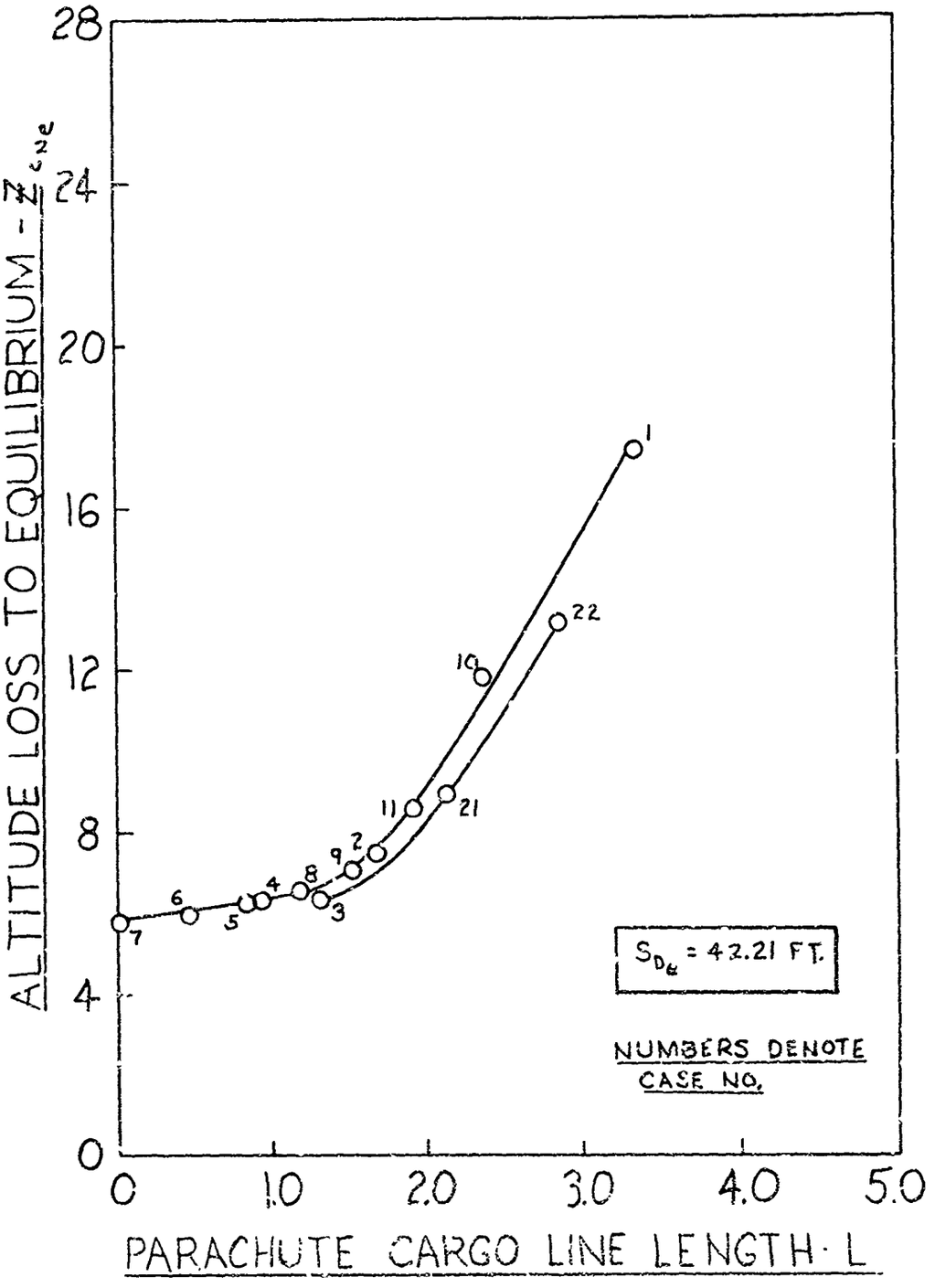

FIGURE 5 - VARIATION OF ALTITUDE LOSS TO EQUILIBRIUM WITH PARACHUTE-CARGO LINE LENGTH

smaller values of the angle or the 95 degree boundary from larger values of the angle. For the asymptotic trajectories, equilibrium is reached by approaching the 85 degree boundary only. A typical asymptotic trajectory and a typical oscillatory trajectory are compared in Figure 6. Figures 5 and 6 show quite well that reduction in parachute-cargo line length offers a fruitful method for lowering airdrop altitudes.

Figure 7 presents the variation in altitude loss to equilibrium with parachute opening time for five parachute-cargo line lengths. Especially noteworthy is the fact that minimum altitude loss to equilibrium occurs at discrete values of parachute opening time. The trajectories calculated for values of ($\tau_f - \tau_r$) that result in minimum altitude loss for a given value of L are characterized by just a slight oscillation about the vertical. For longer opening times, the trajectories become asymptotic in nature and for shorter opening times, the oscillations become more severe. Trajectories for a typically short opening time, an optimum opening time, and a typically long opening time are shown in Figure 8.

In Figure 7, the curve for S_{D_e} = 81.77 resulted from an attempt to determine the effect of increased cargo weight on minimum altitude loss to equilibrium. In six cases, the cargo weight was increased tenfold to 32,500 pounds and the diameter of the single parachute assumed in the mathematical model was increased by a factor of the square root of 8; eight being the number of parachutes actually used for that weight cargo. This resulted in the drag area of the parachute, a function of the square of the

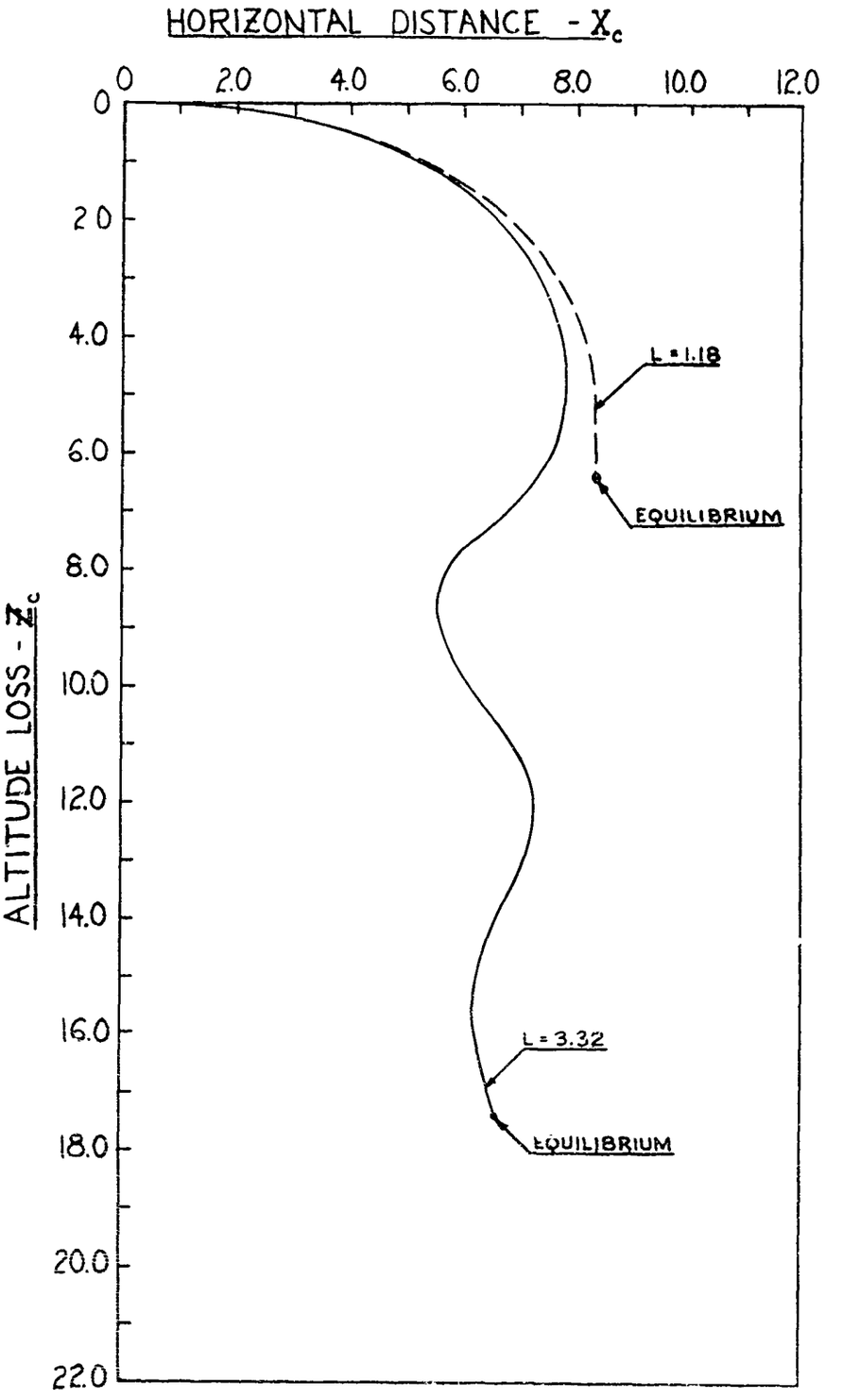

FIGURE 6 - COMPARISON OF CARGO TRAJECTORIES FOR TWO PARACHUTE-CARGO LINE LENGTHS

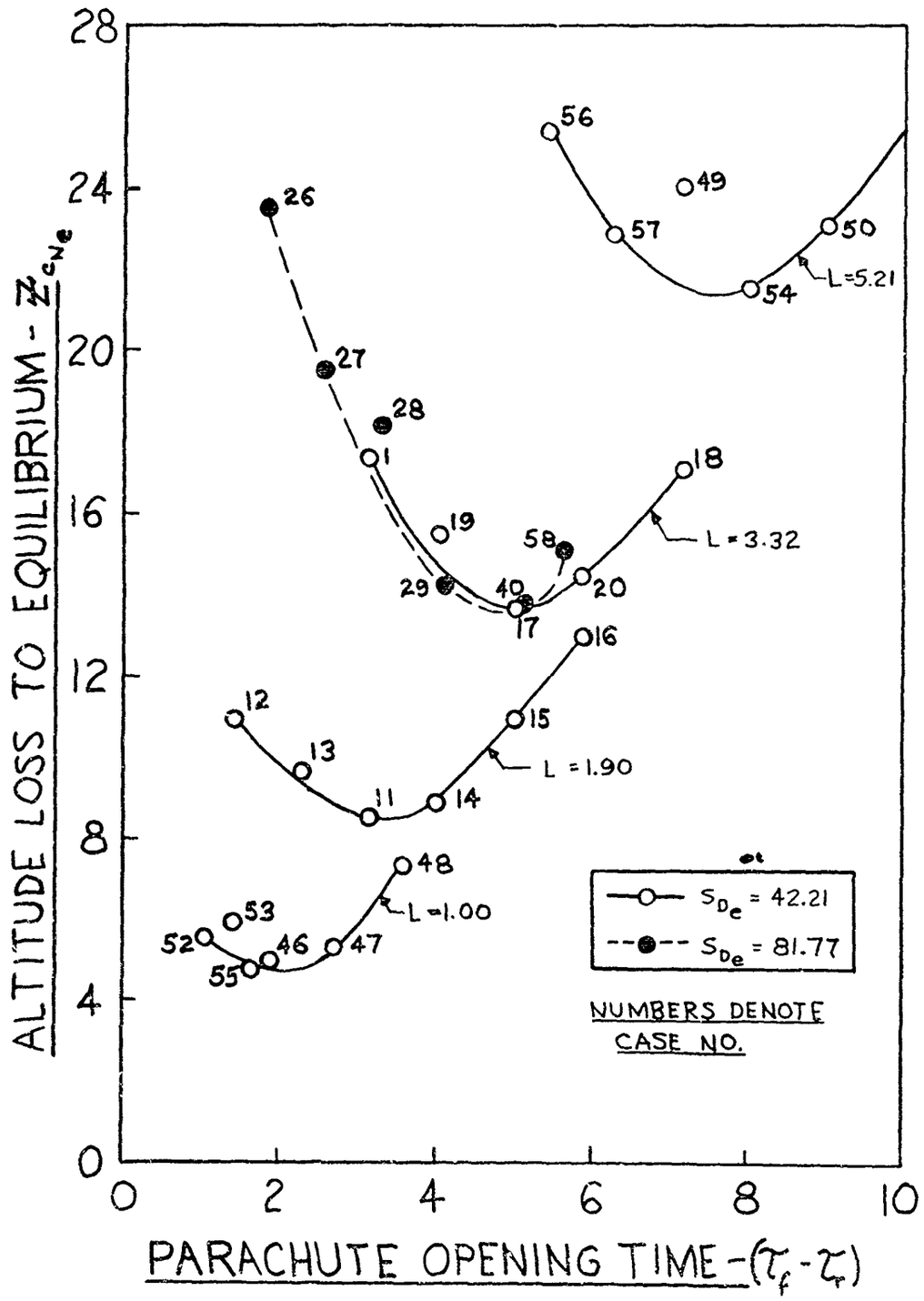

FIGURE 7 - VARIATION OF ALTITUDE LOSS TO EQUILIBRIUM WITH PARACHUTE OPENING TIME

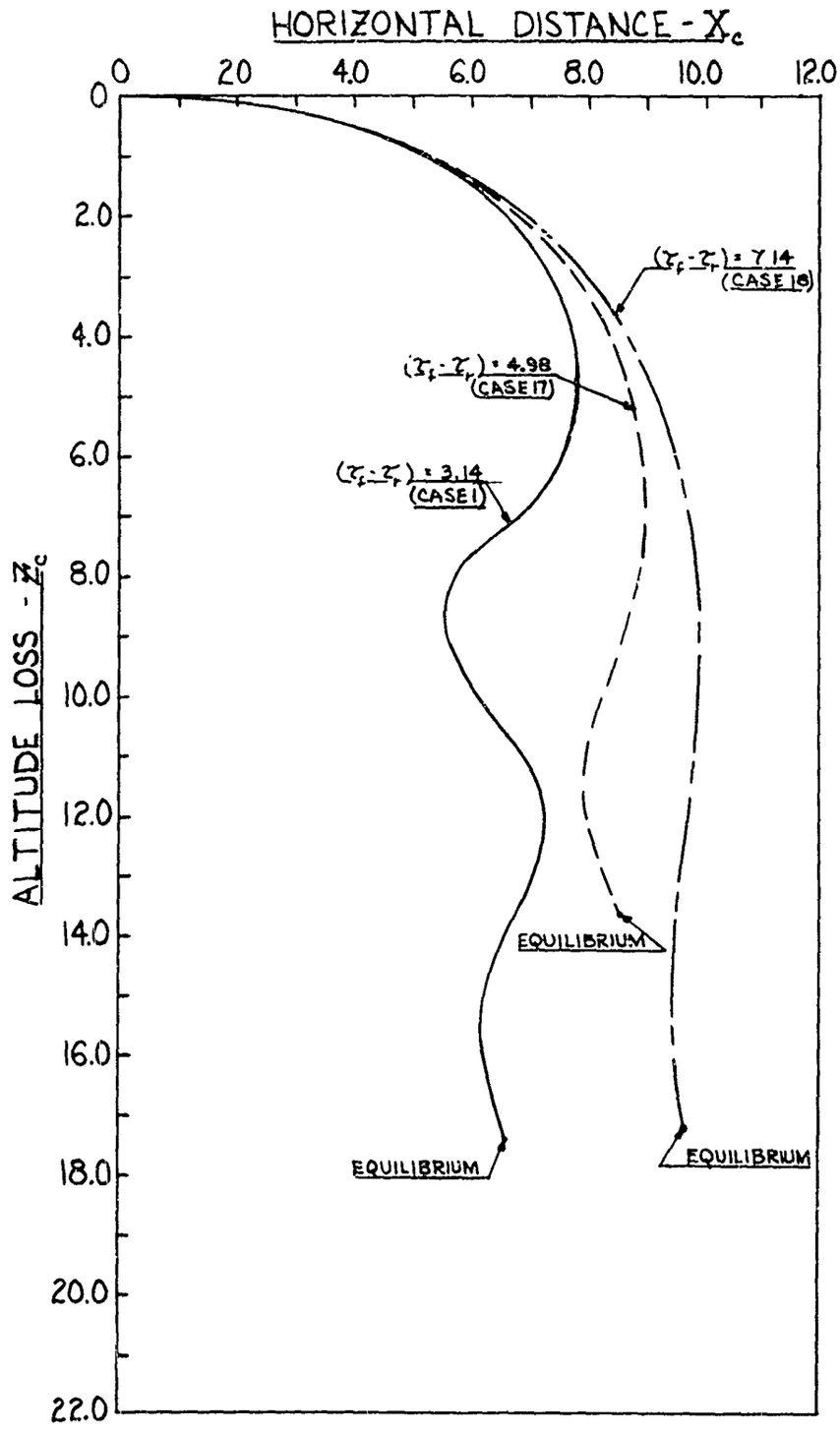

FIGURE 8 - COMPARISON OF CARGO TRAJECTORIES FOR THREE PARACHUTE OPENING TIMES

diameter, being the same as in an actual airdrop. However, the mass of the included air in the parachute is a function of the cube of the diameter. Since the drag area and the included air mass were not increased proportionately, the value for SD_e did not remain constant and, in fact, increased by a factor of almost 2.

Because of this, no specific conclusions can be reached on the effect of increased cargo weight on altitude loss to equilibrium. However a cluster of small parachutes, having the same total drag area as a single large parachute, will have a significantly smaller total mass (and volume) of included air. This should result in shorter opening times, which, as has been shown in Figure 7, may or may not decrease altitude loss to equilibrium. Also, the smaller value of S_{D_e} for the cluster will result in lower values of the non-dimensionalized altitude loss to equilibrium at the optimum parachute opening time. Further, since S_{D_e} is the non-dimensionalizing factor for altitude loss, the smaller value of S_{D_e} will yield even lower values of actual altitude loss to equilibrium. Thus, for a given equilibrium velocity, a cluster of small parachutes with a carefully chosen opening time should permit airdrop from lower altitudes than when using a single large parachute.

The effect of aircraft flight path inclination, at the instant of cargo release, is shown in Figure 9. With the coordinate system used, negative angles indicate that the aircraft is climbing.

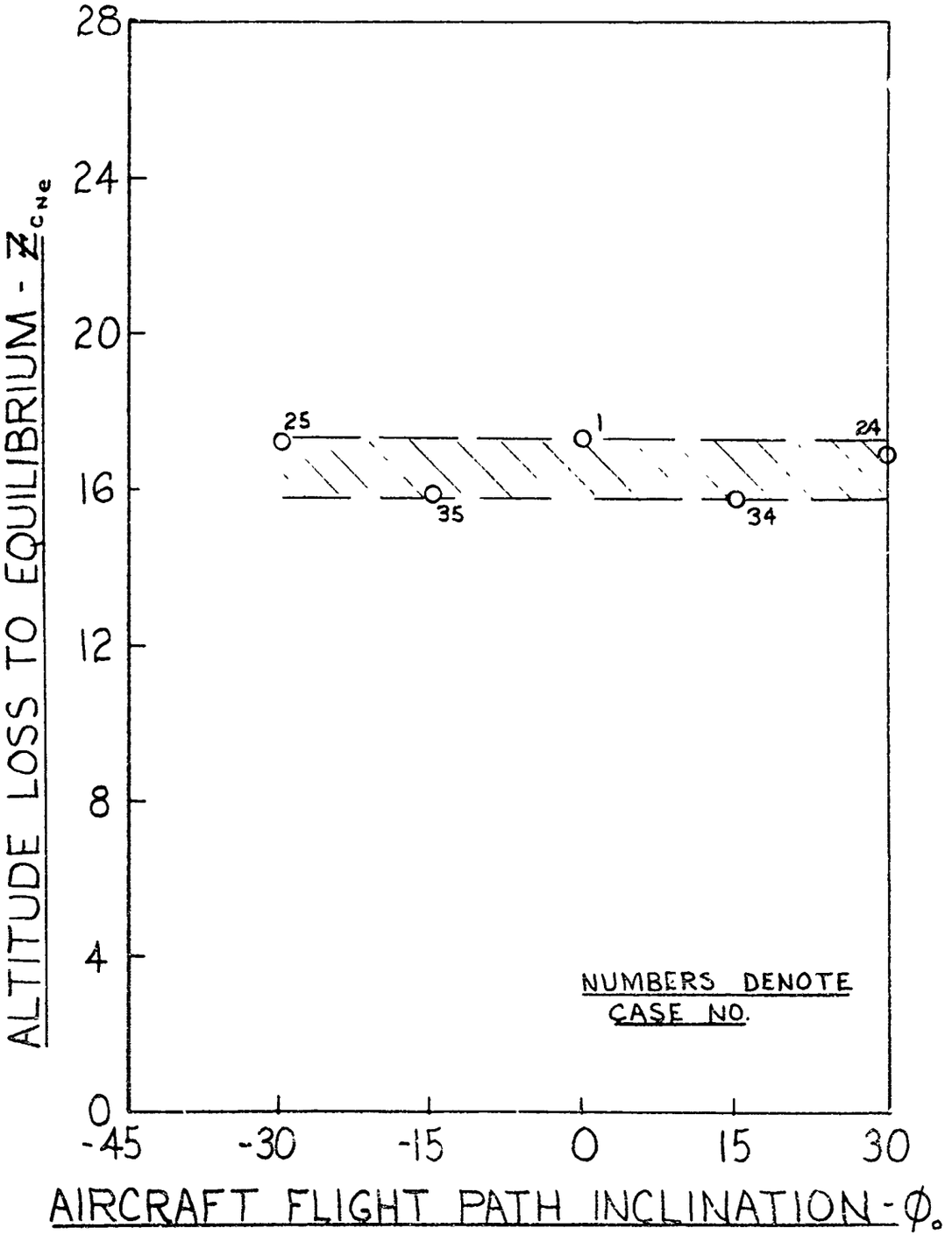

FIGURE 9 - VARIATION OF ALTITUDE LOSS TO EQUILIBRIUM WITH AIRCRAFT FLIGHT PATH INCLINATION

The discontinuity in the curve results from the approach to the equilibrium boundaries changing from one direction to the other. This figure shows that the flight path has no marked effect on altitude loss to equilibrium. Inspection of the cargo trajectories in Figure 10 shows that the trajectories for θ_o equals plus or minus 30 degrees are quite different during the early portions of the trajectories, although they do approach a more typical characteristic during the later portion of their trajectories. For the case of the aircraft in climbing flight, the altitude that the cargo gains during the early portion of the trajectory is almost equivalent to the additional altitude required to damp out the more severe oscillations that result.

The small effects of initial cargo acceleration and initial cargo velocity on altitude loss to equilibrium are shown in Figures 11 and 12. The initial cargo acceleration was calculated by dividing, at time zero, the tension in the line joining the parachute and the cargo by the cargo weight, W_c.

In both figures, the number of cargo oscillations before reaching equilibrium increases step-wise with increasing values of the abscissa, resulting in increasing altitude loss to equilibrium. However, small increases in the value of the abscissa, as long as the number of oscillations is not increased, results in smaller altitude losses to equilibrium. This is especially apparent in Figure 12 and it is felt that the same occurs in Figure 11 although there are not sufficient points to show this conclusively. This "within-the-cycle" phenomenon is due to the

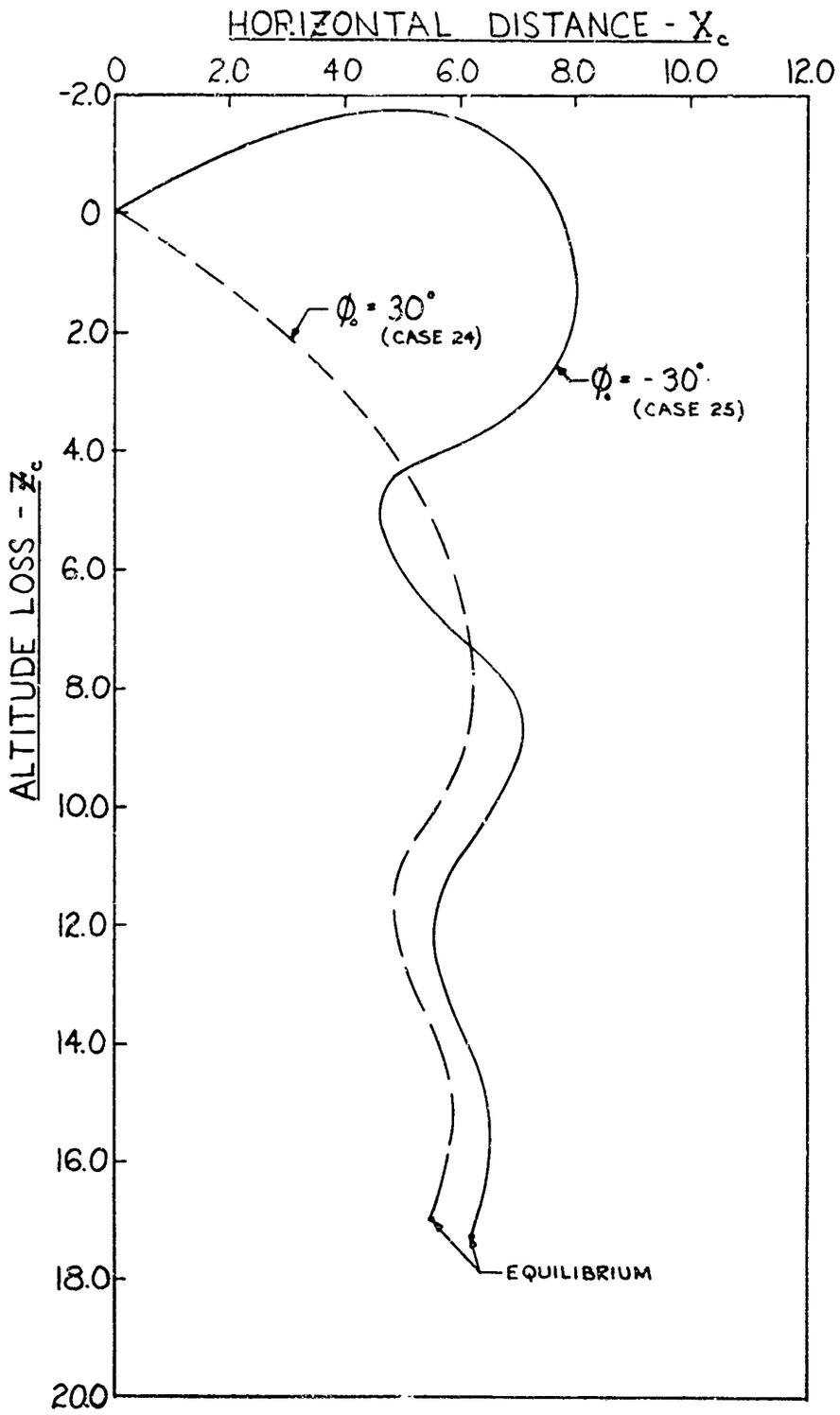

FIGURE 10 - COMPARISON OF CARGO TRAJECTORIES FOR TWO AIRCRAFT FLIGHT PATH INCLINATIONS

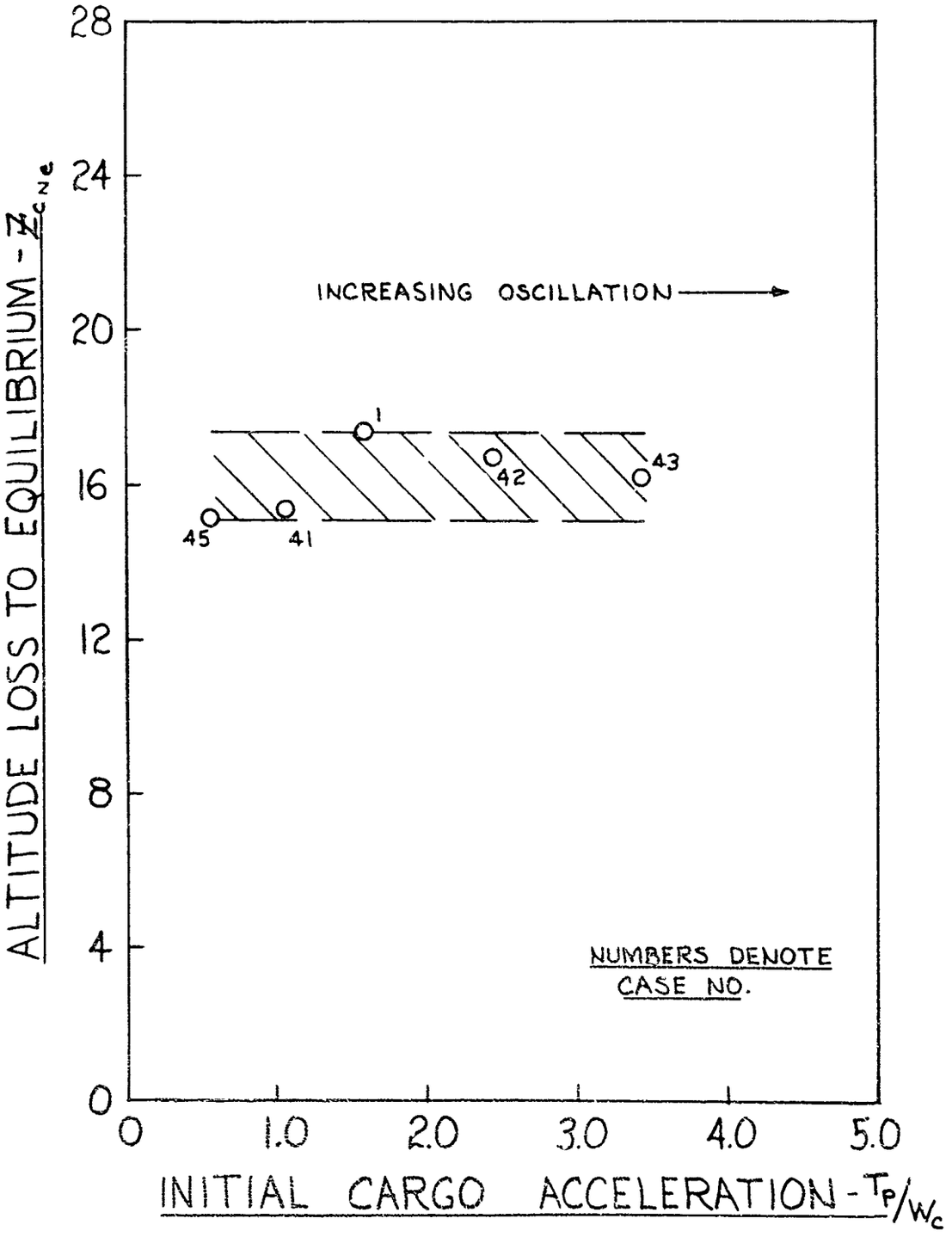

FIGURE 11 - VARIATION OF ALTITUDE LOSS TO EQUILIBRIUM WITH INITIAL CARGO ACCELERATION

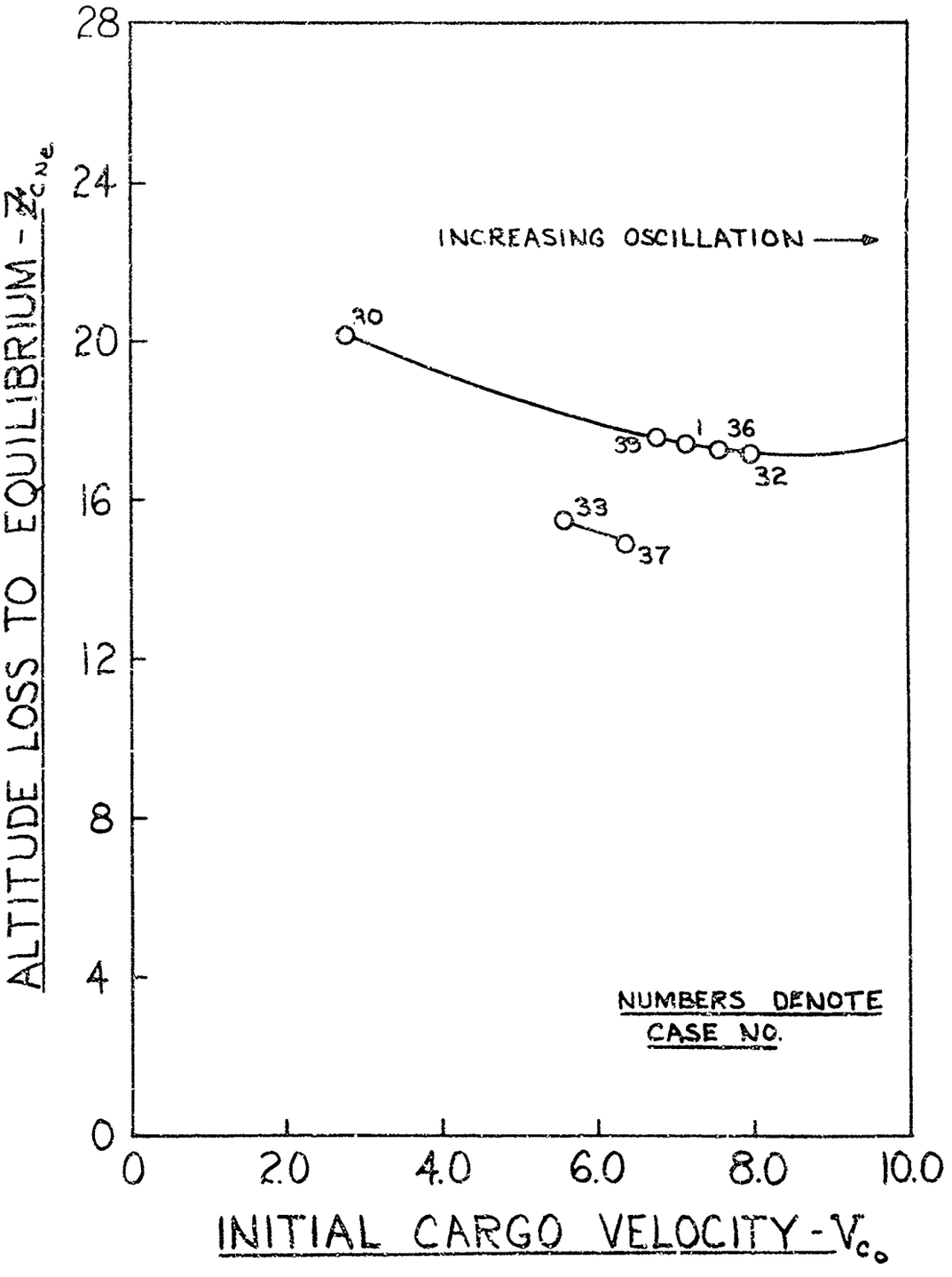

FIGURE 12 - VARIATION OF ALTITUDE LOSS TO EQUILIBRIUM WITH INITIAL CARGO VELOCITY

approaching of the equilibrium boundaries from two directions.

Assessment of the results of this analysis reveals two parameters that significantly affect altitude loss to equilibrium. Those parameters are parachute-cargo line length and parachute opening time. These parameters are closely interrelated and changes in them for any given airdrop system must be accomplished judiciously for as the line length is varied, the value of the optimum filling time changes. Thus, what is optimum filling time for one line length is not optimum for another.

The other parameters that were investigated do not affect altitude loss to equilibrium in sufficient enough degree to warrant special attempts to optimize their values during airdrop system design. This conclusion may be limited in scope since the effects of simultaneous variations of the parameters were not studied. It is suspected that for parachute-cargo line lengths of less than 2.0, where the trajectories are asymptotic in nature and quite different from the nominal case, the effects of initial cargo acceleration, initial cargo velocity and aircraft flight path inclination may be quite different. For instance, it is suspected that, for $L <$ 2.0, increasing initial cargo acceleration will result in decreasing altitude loss to equilibrium rather than the increasing altitude loss shown in Figure 11.

Conclusions

1. The derived equations of motion result in calculated trajectories which are good representations of actual airdrop trajectories.

2. The parameters which most affect altitude loss to equilibrium are parachute-cargo line length and parachute opening time.

3. There is an optimum parachute opening time which results in minimum altitude loss to equilibrium. Longer or shorter opening times will result in greater altitude losses to equilibrium.

4. Moderate variations of aircraft flight path inclination, initial cargo acceleration and initial cargo velocity have only a small effect on altitude loss to equilibrium.

5. For a given equilibrium velocity, a cluster of small parachutes appears to be a better choice than a single large parachute for obtaining minimum altitude loss to equilibrium.

References

1. Patterson, A.G. and J.E. Foster. Low Altitude Air Delivery-Development of Equations of Motion. AAI Corporation, Cockeysville, Md. Report No. ER-4350, April, 1966.

2. Foster, J.E. and B.W. Jezek. Preliminary Investigation of Low Altitude Airdrop Exploratory Development-Extraction by Recovery Parachutes, AAI Corporation, Cockeysville, Md. Technical Report, August, 1966.

3. Neustadt, M., R.E. Ericksen, J.J. Guiteras, and J.A. Larrivee. A Parachute Recovery System Dynamic Analysis. AAI Paper No. 66-25, January 1966.

4. Berndt, R.J. and J.H. DeWeese, Filling Time Prediction Approach for Solid Cloth Type Parachute Canopies. AIAA Aerodynamic Deceleration Systems Conference, Houston, Texas, Sept. 7-9, 1966.

5. Berndt, R.J. Experimental Determination of Parameters for the Calculation of Parachute Filling Times. Annual Meeting WGLR-DGRR, Berlin, Germany, Sept. 1964.

6. Heick, R.J. Performance Characteristics of Standard G-12D and G-11A Cargo Type Parachutes at Overload Conditions. US Army Airborne Test Activity Technical Report T-5, ATA 61035, March, 1962.

7. French, K.E. Inflation of a Parachute. AIAA Journal, Vol. 1, No. 11, Nov, 1963, pp. 2615-2617.

8. Larrabee, E.E. Aerodynamic Penetration and Radius as Unifying Concepts in Flight Mechanics. AIAA Journal of Aircraft, Vol. 4, No. 1, Jan-Feb., 1967, pp. 28-35.

9. Routh, E.J. A Treatise on Dynamics of a Particle. Cambridge University Press, London, 1898.

10. Instructions for RKGS Subroutine, 1130 Scientific Subroutine Package, IBM Application Program, pp. 92-95.

LIST OF SYMBOLS

b	minor semi-axis of oblate hemispheroid
C_D	drag coefficient
D_P	parachute drag
D_{P_o}	parachute diameter when fully open
e_P	eccentricity of oblate hemispheriod
f	length of parachute suspension lines
F	non-dimensional form of f
g	acceleration of gravity
k	spring constant of line joining parachute and cargo
l	length of line joining centers-of-gravity of parachute and cargo
l_r	length of parachute reefing line
Δl	increase in length, due to tension force, of line joining centers-of-gravity of parachute and cargo
L	non-dimensional form of l
m_c	cargo mass
m_{La}	mass of included air in parachute
m_P	total mass of parachute; the sum of canopy mass, included air mass, and additional air mass
m'_P	mass of parachute canopy
M_{La}	non-dimensional form of m_{La}
M_P	non-dimensional form of m_P
M'_P	non-dimensional form of m'_P
r	radius of parachute during opening (major semi-axis of oblate hemispheroid)

r_N	non-dimensional form of r
r_i	inlet radius of parachute during opening
r_{i_N}	non-dimensional form of
R	nominal radius of parachute canopy
S_c	cargo reference area
S_D	aerodynamic penetration
S_p	projected area of parachute
S_{p_o}	projected area of fully open parachute
S_p	non-dimensional form of S_p
t	time
t_f	parachute filling time - measured from line stretch to full open
t_r	time from line stretch to reefed condition
T	tension in line joining parachute and cargo
T_p	tension in line at t = 0
V	velocity
V_r	velocity of cargo with respect to aircraft at t = 0
V	non-dimensional form of V
$Vol._{canopy}$	total volume of par chute canopy
$Vol._{C.F.}$	volume of conical frustum
$Vol._{O.H.}$	volume of oblate hemispheroid
W_c	cargo weight
W'_p	weight of parachute canopy
x	horizontal distance
X	non-dimensional form of x
z	vertical distance (altitude loss)

$\bar{Z}$	non-dimensional form of Z
α	angle of attack
Γ	non-dimensional form of Δl
ϵ	mass ratio
θ	orientation of airdrop system with respect to horizontal
μ	additional mass factor
ρ	air density
τ	non-dimensional form of t
ϕ	angle between velocity vector and horizontal

Subscripts

a	aircraft
c	cargo
e	equilibrium
o	initial condition
p	parachute

Unclassified
Security Classification

DOCUMENT CONTROL DATA - R & D

(Security classification of title, body of abstract and indexing annotation must be entered when the overall report is classified)

1. ORIGINATING ACTIVITY (Corporate author) US Army Natick Laboratories Natick, Mass. 01760	2a. REPORT SECURITY CLASSIFICATION Unclassified 2b. GROUP

3. REPORT TITLE
Two-Body Trajectory Analysis of a Parachute-Cargo Airdrop System

4. DESCRIPTIVE NOTES (Type of report and inclusive dates)
Research Report

5. AUTHOR(S) (First name, middle initial, last name)
Maurice P. Gionfriddo

6. REPORT DATE	7a. TOTAL NO. OF PAGES	7b. NO. OF REFS
April 1969	37	10

8a. CONTRACT OR GRANT NO.	9a. ORIGINATOR'S REPORT NUMBER(S)
b. PROJECT NO. 1F162203D195	69-80-AD
c.	9b. OTHER REPORT NO(S) (Any other numbers that may be assigned this report)
d.	

10. DISTRIBUTION STATEMENT
Distribution of this document has been approved for public release and sale; its distribution is unlimited.

11. SUPPLEMENTARY NOTES	12. SPONSORING MILITARY ACTIVITY
	US Army Natick Laboratories Natick, Mass. 01760

13. ABSTRACT

Equations of motion for a three-degree-of-freedom, two-body airdrop system were derived and numerical solutions obtained by use of a digital computer. It was assumed that, for given initial conditions, the parachute drag area was a function of time only.

The results indicated that:

1. The derived equations of motion result in calculated trajectories which are good representations of actual airdrop trajectories.
2. The parameters which most affect altitude loss to equilibrium are parachute-cargo line length and parachute opening time.
3. There is an optimum parachute opening time which results in minimum altitude loss to equilibrium. Longer or shorter opening times will result in greater altitude losses to equilibrium.
4. Moderate variations of aircraft flight path inclination, initial cargo acceleration, and initial cargo velocity have only a small effect on altitude loss to equilibrium.
5. For a given equilibrium velocity, a cluster of small parachutes appears to be a better choice than a single large parachute for obtaining minimum altitude loss to equilibrium.

DD FORM 1 NOV 68 1473 REPLACES DD FORM 1473, 1 JAN 64, WHICH IS OBSOLETE FOR ARMY USE.

Unclassified
Security Classification

14 KEY WORDS	LINK A		LINK B		LINK C	
	ROLE	WT	ROLE	WT	ROLE	WT
Equations of motion	8					
Trajectories	9					
Parachute Descent	9					
Cargo Parachutes	9		9			
Air drop operations	4		4			
Length			6			
Parachute lines			6			
Opening			6			
Time			6			
Parachutes			6			
Altitude loss			7			
Equilibrium			7			
Cluster parachutes			6			